

REPORT DOCUMENTATION PAGE

AFRL-SR-AR-TR-02-

Public reporting burden for this collection of information is estimated to average 1 hour per response, including gathering and maintaining the data needed, and completing and reviewing the collection of information. Send collection of information, including suggestions for reducing this burden, to Washington Headquarters Services, Directorate for Information Operations and Reports, 1215 Jefferson Davis Highway, Suite 1204, Arlington, VA 22202-4302, and to the Office of Management and Budget, Paperwork Project, Washington, DC 20503.

0341

| | | |
|--|--|---|
| 1. AGENCY USE ONLY (Leave blank) | 2. REPORT DATE 17 SEP 02 | 3. REPORT TYPE AND DATES COVERED FINAL REPORT 15 JAN 01 TO 31 MAR 02 |
| 4. TITLE AND SUBTITLE Nanocomposite and Photonic-Crystal Polymer Structures for Nonlinear Photonic Applications | | 5. FUNDING NUMBERS F49620-01-1-0135 2303/CV 61102f |
| 6. AUTHOR(S) Dr L. Jay Guo | | |
| 7. PERFORMING ORGANIZATION NAME(S) AND ADDRESS(ES) University of Michigan Dept of Electrical Engineering 3411 EECS, Dept 1301, Beale Avenue Ann Arbor, MI 48109-2122 | | 8. PERFORMING ORGANIZATION REPORT NUMBER |
| 9. SPONSORING/MONITORING AGENCY NAME(S) AND ADDRESS(ES) AFOSR/NL 4015 Wilson Blvd., Room 713 Arlington, VA 22203-1954 | | 10. SPONSORING/MONITORING AGENCY REPORT NUMBER |
| 11. SUPPLEMENTARY NOTES | | |
| 12a. DISTRIBUTION AVAILABILITY STATEMENT Approve for Public Release; Distribution Unlimited | | 12b. DISTRIBUTION CODE |
| 13. ABSTRACT (Maximum 200 words) We have developed two experimental techniques for creating photonic structures in nonlinear optical (NLO) polymers with precisions down to nanoscale. The first technique uses nanoimprinting technology to directly pattern the guest-host NLO polymers. It can be applied to the fabrication of photonic bandgap structures in NLO materials, as well as many other photonic structures in both linear and nonlinear polymers. For example, we have shown that micro-ring optical resonator structure can be fabricated by using the imprinting technique. The second technique utilize self-assembly of NLO polymer monolayers onto nanostructured template. This approach provides a highly effective means to implement waveguide devices using high performance self-assembled polymers with large electro-optic activity and inherent long-term stability. Such method can also be extended to Langmuir-Blodgett (LB) and covalently self-assembled thin films, and enables practical device applications for nonlinear optical thin films synthesized by these different layer-by-layer growth approaches to utilize their material properties, such as high nonlinear optical coefficient, very fast electronic response and good thermal and temporal stability. | | |
| 14. SUBJECT TERMS 20021031 015 | | 15. NUMBER OF PAGES |
| | | 16. PRICE CODE |
| 17. SECURITY CLASSIFICATION OF REPORT Unclass | 18. SECURITY CLASSIFICATION OF THIS PAGE Unclass | 19. SECURITY CLASSIFICATION OF ABSTRACT Unclass |
| 20. LIMITATION OF ABSTRACT | | |

Final Project Report

For AFOSR Grant F49620-01-1-0135

Nanocomposite and Photonic-Crystal Polymer Structures for Nonlinear Photonic Applications

Principle Investigator: L. Jay Guo

*Solid-State Electronics Laboratory
Department of Electrical Engineering and Computer Science
Macromolecular Science and Engineering, & Applied Physics
University of Michigan, Ann Arbor, MI 48109-2122*

Subcontractor

Professor Robert Boyd

*Institute of Optics
University of Rochester
Rochester, NY 14627*

Total budget: \$140,000

Funding period: January 2001— December 2001

(No-cost extension to March 2002)

DISTRIBUTION STATEMENT A

Approved for Public Release
Distribution Unlimited

Nanocomposite and Photonic-Crystal Polymer Structures for Nonlinear Photonic Applications

L. Jay Guo

Solid-State Electronics Laboratory
Department of Electrical Engineering and Computer Science
Macromolecular Science and Engineering, & Applied Physics
University of Michigan, Ann Arbor, MI 48109-2122

1. Summary of research accomplishment

We have developed two experimental techniques for creating photonic structures in nonlinear optical (NLO) polymers with precisions down to nanoscale. The first technique uses nanoimprinting technology to directly pattern the guest-host NLO polymers. It can be applied to the fabrication of photonic bandgap structures in NLO materials, as well as many other photonic structures in both linear and nonlinear polymers. For example, we have shown that micro-ring optical resonator structure can be fabricated by using the imprinting technique. The second technique utilize self-assembly of NLO polymer monolayers onto nanostructured template. This approach provides a highly effective means to implement waveguide devices using high performance self-assembled polymers with large electro-optic activity and inherent long-term stability. Such method can also be extended to Langmuir-Blodgett (LB) and covalently self-assembled thin films, and enables practical device applications for nonlinear optical thin films synthesized by these different layer-by-layer growth approaches to utilize their material properties, such as high nonlinear optical coefficient, very fast electronic response and good thermal and temporal stability. We have also developed techniques to fabricate polymer micro-ring resonator devices, and very recently demonstrated its operation. These works have been reported in two conferences and 3 refereed journal articles will be published. Professor Boyd's group at University of Rochester has developed a new measurement technique for characterizing the NLO material, and investigated enhanced fluorescence from a microstructured surface that is fabricated by the University of Michigan.

In addition to these experimental achievements, we have also investigated a number of novel photonic devices by simulation and modeling. Three types of devices are reported here, all of which can be fabricated by using a combination of the experimental techniques developed under this grant. We have designed and modeled a microring resonator device made of nonlinear optical (NLO) polymer for all-optical switching application. In this device NLO polymer provides the saturable absorption nonlinearity and microring resonator provides the feedback needed for optical bistability. Waveguide confinement and field intensity build-up in the ring resonator both facilitate the nonlinear optical process, making it possible to achieve low switching intensity. This work is to be published in the SPIE proceedings. We have also proposed an optical switching device based on resonate grating waveguide structure using nanoimprinted NLO polymers. Because the resonant grating structure has highly sensitive frequency selectivity, an optical switch can be implemented by choosing the grating material to have intensity dependent refractive index. Very recently, we have investigated a Si photonic bandgap (PBG) structure incorporating EO polymer using Finite Difference Time Domain (FDTD) method, and our simulation shows that such a device can function as a tunable filter or as a compact EO modulator. The common feature of all these proposed microphotonic devices is that they are highly compact in dimension with

respect to their functionality, and represent the first step in utilizing EO or NLO polymers in microresonator or PBG structures for photonic applications.

2. Details of Technical Achievements

Polymeric nanostructures potentially has important applications in making useful integrated optic systems. A fabrication technique that is able to create nanoscale structures in NLO polymers will allow us to explore a number of interesting phenomenon as well as important device applications. One example is photonic crystals, or photonic bandgap (PBG) materials, which provide entirely new means of light confinement, guiding, and routing by using a linear periodic media [1]. However, it is expected that nonlinear PBG structure offers much richer and more complex response to light interaction with the periodic NLO media.

We have developed two experimental techniques for creating photonic structures in nonlinear optical (NLO) polymers with precisions down to nanoscale. The first technique uses nanoimprinting, a new technology that can form nanoscale structures in polymers. We show that it can directly pattern photonic crystal structures in guest-host NLO polymers cast on a substrate [2]. The second technique is electrostatic self-assembly of NLO polymers in nanofabricated template to form ordered NLO polymer structures [3]. This approach provides a highly effective means to implement practical waveguide devices using high performance self-assembled polymers with large electro-optic activity and inherent long-term stability.

2.1. NLO Polymer structures fabricated by Nanoimprinting

We have developed a technology over the past few years, called nanoimprinting, which is especially suitable for fabricating nanoscale photonic structures in polymers. Nanoimprinting utilizes a hard mold with pre-defined nanoscale features to mechanically imprint into a polymer film cast on a substrate, while the polymer is heated to above its glass transition temperature (T_g). The thickness contrast pattern thus created is "frozen" into the polymer during a cooling cycle. Originally conceived as a technique for nanopatterning [4], nanoimprinting has demonstrated the capability of creating patterned polymer structures with high throughput and sub-10 nm resolutions [5]. Now we show that it is straightforward to apply nanoimprinting to fabricate photonic nanostructures in guest-host NLO polymers. Figure 1 illustrates the procedure: a pre-patterned structure (in this case, a 1D grating) is first fabricated on a master mold by using lithography and reactive ion etching [4, 5, 6]. The mold is pressed into a NLO polymer by mechanical force while both the substrate and the mold are held at a temperature above T_g . If it is desired that the patterned polymer to have $\chi^{(2)}$ nonlinear response, an electric field can be applied at the same time to align the chromophores in the host polymer so as to

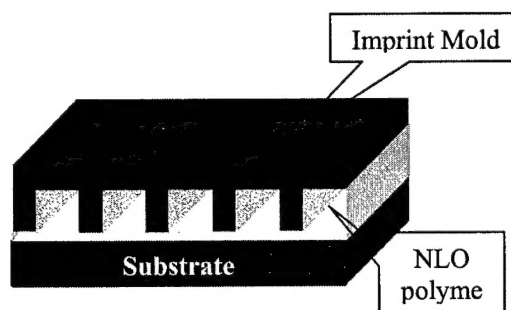


Fig. 1 Fabrication of NLO polymer structure by using nanoimprinting.

induce a noncentrosymmetric configuration necessary for second-order nonlinearity. After the mold and the substrate are cooled down to room temperature the mold is separated from the NLO polymer, leaving a complimentary pattern in the NLO polymer layer. Creating a PBG structure in a third-order NLO polymer is simpler because the electric poling process can be omitted. It is expected that almost any guest-host polymeric NLO systems can be patterned into PBG structures in this fashion.

Planar PBG structures typically involve large areas of sub-wavelength periodic features in 1D or 2D, which makes nanoimprinting an ideal technology for such material structures. The process can be repeated an indefinite number of times as long as the mold is not damaged. As another example, PBG waveguide using a line defect in a polymer PBG structure is only a matter of creating a proper mold with certain columns removed. Therefore this fabrication procedure not only provides a convenient way of incorporating many existing NLO polymers into interesting device structures, but also can be further developed to become a low cost manufacturing technology.

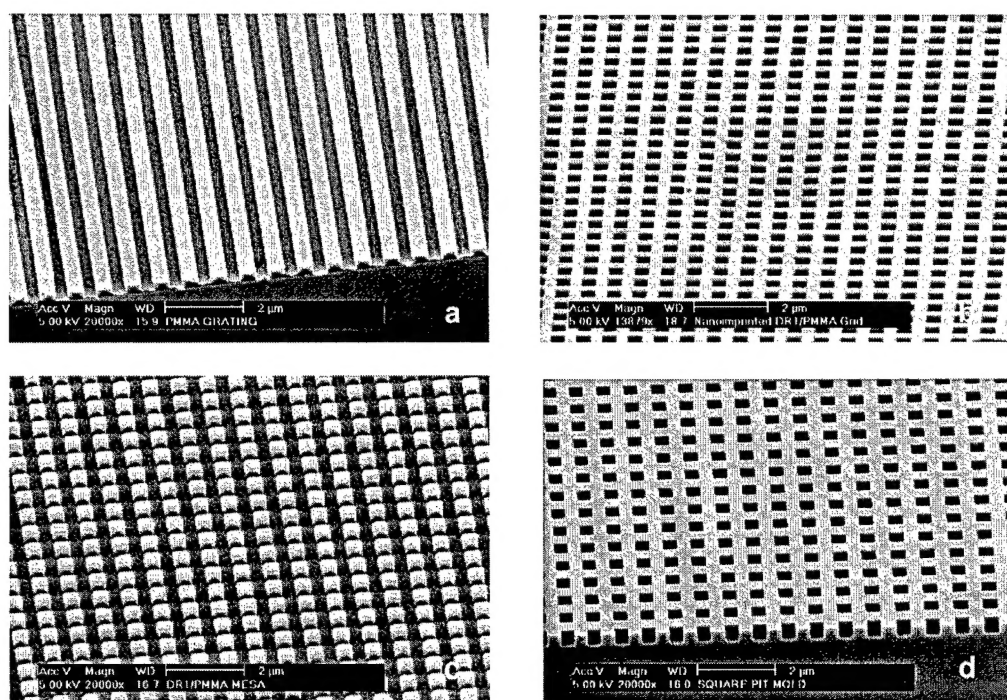


Fig. 2 Scanning electron micrographs of nanoimprinted 700 nm period (a) DR1-PMMA gratings (b) 2D air hole arrays in DR1-PMMA (c) 2D pillar arrays of DR1-PMMA, and (d) the mold fabricated in SiO_2 for producing the pattern in (c).

We have experimented using nanoimprinting approach to create PBG structures in Disperse Red 1 - (DR1) doped Poly(methyl methacrylate) (PMMA). PMMA is a widely used optical host polymer and is perfectly compatible with nanoimprinting process. DR1 is a common NLO dye, and the nonlinear properties of DR1-doped PMMA system have been well characterized. We have imprinted successfully 1D and 2D periodic structures in DR1/PMMA polymer. Figure 2a and 2b show a 700 nm period grating and a 2D air hole arrays created in DR1/PMMA. Figures 2c and 2d show 2D arrays of DR1/PMMA NLO

polymers pillars and the mold used to produce such a pattern respectively. We have used a temperature of 175 °C for 5 minutes during imprinting, and maintained a pressure of about 5 MPa till the sample is cooled to 50 °C, and finally the mold is separated from the substrate at room temperature. We are currently using the DR1/PMMA polymer for a range of proof-of-concept device structures, such as to study the enhanced nonlinear phase shift of light propagation through NLO PBG structures that was theoretically predicted [7], as well as using PBG structure as a means to modify and enhance the electro-optic (EO) properties of current EO polymer materials.

We would like to point out that the imprinting technique itself is not limited to making periodic structures. In fact it can be used like a lithography tool to generate any patterned features. In addition, it offers another useful feature in that it can create polymer structures with different height profiles. With such flexibility, for example, one can “stamp out” a polymer waveguide with a surface relief grating in a single step. It is also frequently observed in our experiments that etched molds has much smoother surface than etched polymer surfaces. The reason may be that the mold is fabricated from hard and highly homogeneous material such as thermally grown SiO₂, and it is usually etched with slower rate. Consequently, the polymer structure transferred from the mold by the conformal imprinting process has smoother surfaces than the etched one. This could significantly reduce the scattering loss due to surface roughness, which is one of the most important loss mechanisms in optical polymer structures.

2.2. Self-Assembly of EO polymers onto patterned template for enhanced thermal and temporal stability

It has long been recognized that the challenge in using poled polymers for practical integrated electro-optic devices is the stability of the acentric alignment of NLO chromophores, which often degrades the material's EO activity over the time. To overcome this problem, several synthetic methods have been developed to aim at fixing the chromophore orientation at molecular levels. These are molecular self-assembly approaches using strategies such as structural interlocking of the dipolar molecules into cone-shaped supermolecules [8], or covalent self-assembly process in which acentric chromophore superlattices are built up in a layer-by-layer fashion [9, 10]. Such techniques are highly promising because the orientation of the chromophore dipoles are permanently fixed by molecular bonding, which guarantees the film's thermal and temporal stability and eliminate the electric poling. In addition, the molecular building block can be tailored and engineered to give rise to very large EO coefficient. However, because each self-assembled monolayer is on the order of 1 nm thick, construction of any practical device structure with film thickness on the order of a micron could be extremely time-consuming, which placed a serious hurdle for practical device applications. As a result, typically only a very thin active layer is used in an EO modulator device, which greatly depreciates the potential of these high-performance EO polymers.

A nanopatterned dielectric template, however, offers the possibility to put the self-assembly approach to practical use. For example, if a dielectric grating is first fabricated, EO materials can then be self-assembled onto this grating template. Not only can this approach be used to produce periodic EO polymer structures with long term stability, but more importantly it would allow rapid build-up of a significantly thick layer for wave guiding in integrated electro-optic devices. We propose a Mach-Zehnder EO modulator structure (a schematic shown in figure 3), where the arms are segmented waveguide having nanoscale gratings along the wave propagation direction. The transverse dielectric grating will act as a

template for self-assembling EO polymers on the sidewalls to fill in the grating trenches. In such a construct the waveguide dimension is essentially set by the pre-patterned grating template. Since the grating spacing is very small, only a thin layer of self-assembled EO polymer is needed, which greatly shortens the time to create a waveguide that contains a large fraction of the active EO material. Furthermore, the chromophore dipole moments are aligned perpendicular to the grating grooves, so a pair of modulating electrodes placed next to this composite waveguide would maximize the overlap integral between the modulating RF fields and the propagating light-field inside the waveguide, resulting to efficient EO modulation.

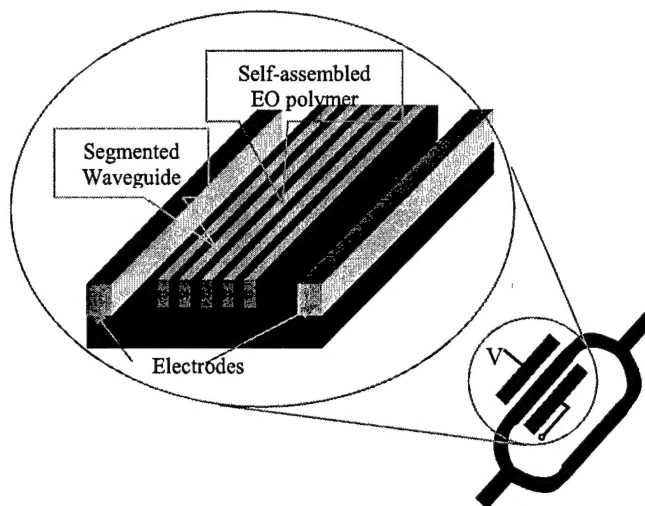


Fig. 3. Schematic of a Mach-Zehnder modulator with arms made of transverse segmented waveguides that are composed of nanoscale dielectric gratings and the EO polymers self-assembled within the grating trenches.

As an initial test of this idea, we have developed a technique to fabricate periodic NLO structures by growing electrostatic self-assembled monolayers onto a grating template (figure 4). Electrostatic self-assembly is an emerging technology that can create nanocomposite polymers with tailored material properties [11]. Such self-assembly process is based on the electrostatic interactions between polycation and polyanion layers that are deposited in alternating steps. By incorporating functional groups to the

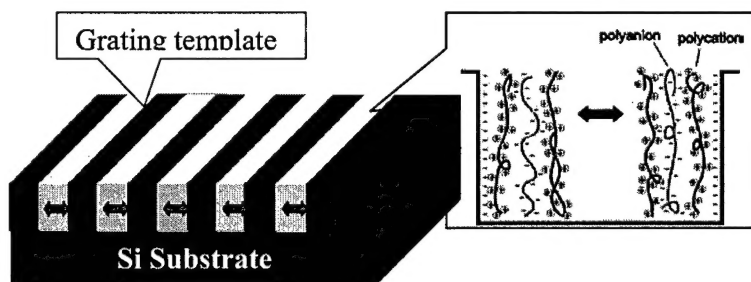


Fig. 4 Schematic diagram of ionically self-assembled bilayers on grating template (arrows indicating the chromophore dipole alignment direction).

polymer chains, one can achieve various desired material functionalities. Nonlinear optical polymeric materials with azo-chromophore can be used as a component to form NLO composite material [12]. The internal field created by the ionic charges naturally aligns the chromophore dipole moment approximately perpendicular to the growth direction, eliminating the need of electrical poling for $\chi^{(2)}$ nonlinearity [12]. The stability of the film is also enhanced by the ionic bonds between the neighboring layers.

In our experiment, we used a grating sample as a template to control the growth of electrostatic self-assembled EO polymer, where growth occurs on the sidewalls of the grating grooves. The SiO_2 grating with 700 nm period and approximately 50% duty cycle is fabricated from a mold by nanoimprinting

lithography and reactive ion etching. The sample is then cleaned with piranha solution ($\text{H}_2\text{O}_2:\text{H}_2\text{SO}_4 = 3:7$), which helps the formation of $-\text{OH}^+$ groups on SiO_2 surface. The positive H^+ ions can be readily exchanged with other cations in a polyelectrolyte solution. We used Poly(diallyldimethylammonium chloride) (PDDA) as polycation and poly dye s-119 as polyanion. Poly dye s-119 contains azo-chromophore group that exhibits nonlinear optical properties. Bilayers are formed by alternately dipping the sample into PDDA, DI water and poly s-119 solutions. The sequence is repeated and a thick layer is build up on the grating sidewalls. The SEM micrographs (figures 5a and 5b) show that the sidewalls of SiO_2 grating after film growth remain very smooth. SEM micrographs (figures 5c to 5d) also show the width of grating gap is reduced from the initial 370 nm to 310 nm after 20 growth cycles, and 250 nm after 40 cycles. Each bilayer has a thickness of ~ 1.5 nm. The film growth and its uniformity are also confirmed by UV-Vis absorption spectra of the same number of bilayers grown on a glass slide. We believe that this scheme can be equally applied to the covalently self-assembled EO polymers, which opens the door for many practical device applications where nanocomposite materials are synthesized by self-assembly method.

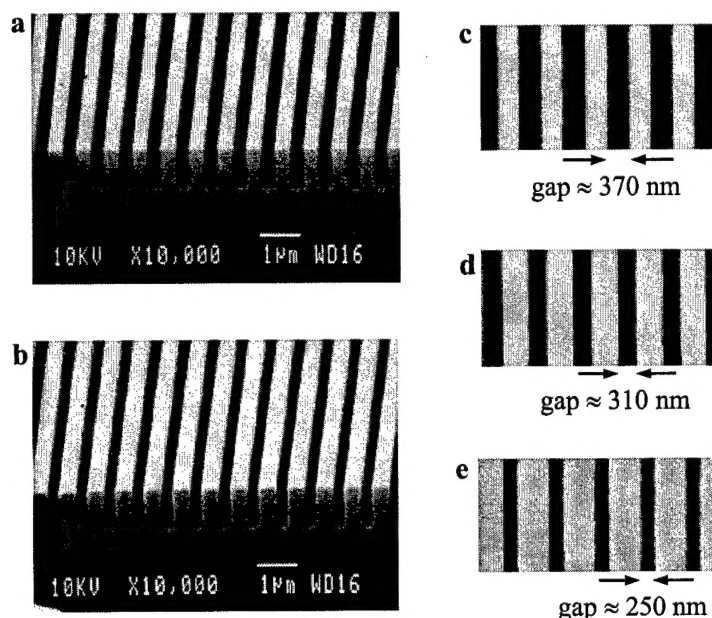


Fig. 5 SEM micrographs of the initial SiO_2 gratings (a) and after 20 ionic self-assembly cycles (b); c, d and e are top views of SiO_2 grating after 0, 20, and 40 self-assembly cycles respectively, showing progressive closing the grating trenches.

2.3. Nonlinear microring resonators for optical switching applications

Ultrafast all-optical switching device will play an important role in future optical communications. In optical fiber systems, optical bistability effect (Fig. 6a) in fiber ring structures based on Kerr effect [13] or saturable absorption effect [14] has been proposed and experimentally demonstrated [15]. Recently Rrof.

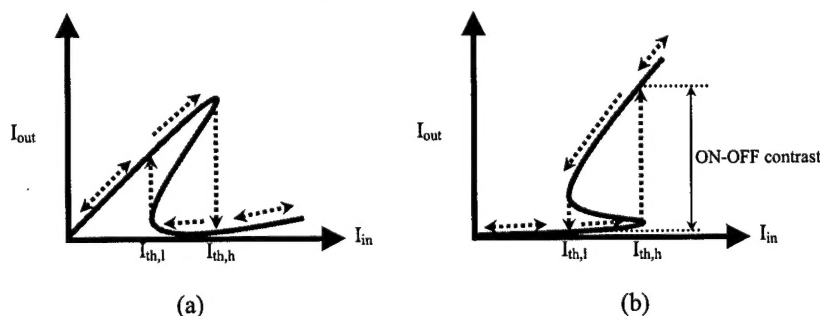


Fig. 6. Schematics of two types of optical bistable behavior.

Boyd's group at Univ of Rochester has proposed a nonlinear fiber optic Mach-Zehnder interferometer device [16] where a fiber-ring resonator is coupled to one arm, and it was predicted

that the device possesses a switching threshold that is reduced by a factor about the square of the finesse of the resonator. But use of fiber-ring resonator with large circumference L will seriously limit time response of the device, because the inherent transient time of the resonator is determined by the cavity lifetime, which is directly proportional to L . Based on our initial result that polymer micro-disk and micro-ring structures can be fabricated by nanoimprinting technique, we propose an integrated waveguide microring resonator device, and use saturable absorption nonlinearity to achieve optical bistability. NLO polymers having conjugate π -electron chromophores oftentimes have very large nonresonant NLO coefficients, and the time response is also ultrafast [17].

In microrings, not only are the optical fields confined in the optical waveguides, but also their intensity build up in the resonator. Such enhancement is highly desirable for nonlinear optical effect. We showed that by using a microring coupled with two waveguides, an "S" shaped bistable curve (Fig. 1b) can be obtained, which is more useful for optical switching application. Moreover, due to large optical nonlinearity of the NLO polymer and the microring resonator characteristics, the device size can be shrunk down to several tens of microns. The small geometry not only provides high-degree of integration, but also increases the switching speed. Here we briefly report the operation principle of a microring resonator, and the design of optical switching device using saturable absorption properties, detailed

discussion will be published in SPIE [18].

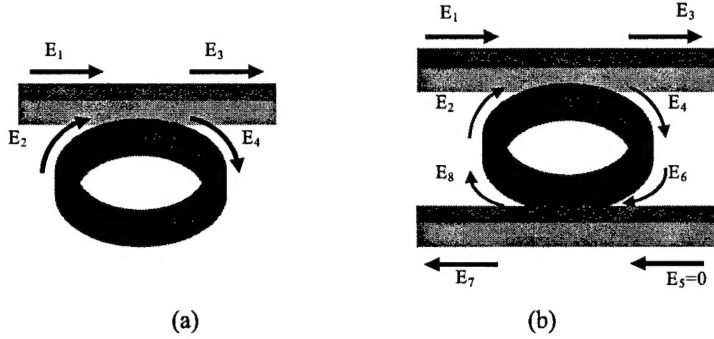


Fig. 7. Two types of nonlinear microring resonant structure.

We have considered two configurations for the design of the device, as shown in Fig. 7. In the first configuration, a waveguide is coupled with a microring (Fig. 7a). The input field (E_1), output field (E_3) and circulating field inside the ring (E_2 and E_4) can be described by the following coupled-mode equations⁴

$$\begin{aligned} E_3 &= \alpha_i (\tau E_1 + j\kappa E_2) \\ E_4 &= \alpha_i (j\kappa E_1 + \tau E_2) \end{aligned} \quad (1)$$

where τ is the amplitude transmission coefficient, κ is the amplitude coupling coefficient and α_i is the insertion loss due to the waveguide mode mismatch in the coupling region. The transmission at resonance is found to be

$$T = \frac{I_3}{I_1} = \frac{|\alpha_i \tau - a|^2}{|1 - a(\alpha_i \tau)|^2}, \quad (2)$$

where a is the single-pass amplitude attenuation factor: $E_2 = ae^{i\phi}E_4$. Transmission drops to zero as a is close to $\alpha_i \tau$. In contrast, it increases as a is away from $\alpha_i \tau$. A typical plot of transmission as a function of a is shown in Fig. 8a.

In the second configuration (Fig. 7b), a microring is coupled with two waveguides, one acting as input and output port (E_1 & E_3), and the other as drop port (E_7). Similar derivation procedures can be

followed. Defining $E_6 = a_1 e^{j\phi/2} E_4$ and $E_2 = a_2 e^{j\phi/2} E_8$ together with two sets of coupled equations leads to the output transmission at the drop port, defined as the ratio of I_7 to I_1 , at resonance

$$T_{drop} = \frac{I_7}{I_1} = \left| \frac{a_1 \alpha_i^2 \kappa^2}{1 - (a_1 a_2 \alpha_i \tau) \cdot (\alpha_i \tau)} \right|^2 \quad (3)$$

where a_1 and a_2 are, respectively, the half-pass amplitude attenuation factors of the right and left parts of the microring. A typical plot of T_{drop} as a function of a_1 ($= a_2$) is shown in Fig. 8b.

The single- and half-pass amplitude attenuation factors, a , a_1 and a_2 that appear in Eqs. (2) and (3) include the material absorption loss and all other radiation losses in the microring waveguide, such as scattering loss caused by surface roughness, substrate loss and bending loss. Fig. 8a and Fig. 8b both indicate that a switching device can be implemented by controlling

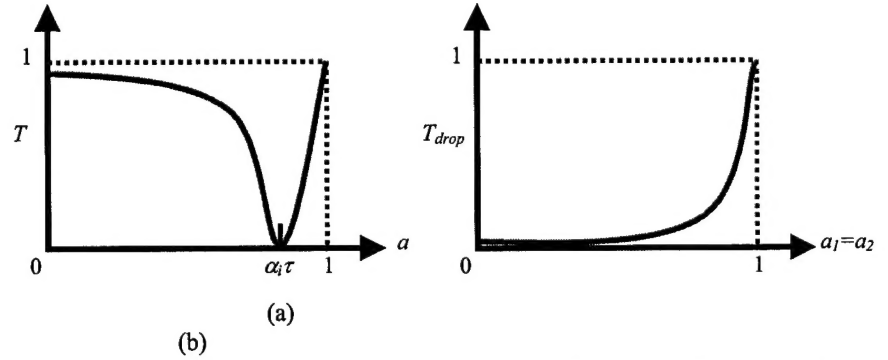


Fig. 8. (a) A typical transmission curve of the case in Fig. 7a as a function of the single-pass amplitude attenuation; (b) typical transmission curve of the case in Fig. 7b as a function of the half-pass amplitude attenuation with a_1

the absorption loss in the microring. We would like to use saturable absorption nonlinearity to control the absorption loss in the microring and to implement an all-optical switch. Saturable absorption is a type of $\chi^{(3)}$ nonlinear optical phenomena, which results in an intensity-dependent absorption coefficient

$$\alpha(I) = \frac{\alpha_0}{1 + \frac{I}{I_s}} \quad (4)$$

where α_0 is the unsaturated absorption coefficient, I the local field intensity and I_s the saturation intensity.

The design of a microring optical switch using bistability should be such that the switching intensity, $I_{th,h}$, is small, the switching window, $I_{th,h} - I_{th,l}$, is small and the ON-OFF contrast is large to approach an ideal switch (see the definitions in Fig. 1b). Using detailed modeling we have shown how the values of several parameters, α_0 , τ , α_c , α_l and m should be chosen in order to satisfy these requirements. In principle, optical bistability is caused by two factors: nonlinear mechanism of the media and optical feedback. In our case, saturable absorption provides optical nonlinearity and a microring resonator offers feedback path. Among these parameters, α_0 determines the strength of saturable absorption, and coupling coefficient, κ , (and hence $\tau = \sqrt{1 - \kappa^2}$) determines the amount of light coupled into the microring feedback loop. Therefore, these two parameters are the most significant ones in the design. The influences of other parameters are less significant, but should be optimized to enhance the device performance. Simulated optical bistability behavior of the NLO microring devices are shown in Fig. 9, which address the different roles of the aforementioned parameters. Clearly an optical switch can be implemented using nonlinear microring resonators with saturable absorption properties. Among various parameters, α_0 and I_s are determined by the material properties. α_c and α_l are determined by waveguide design and fabrication. α_0 should be properly chosen because of the trade-off between contrast and switching intensity as well as

output intensity. As for I_s , it should be as small as possible to reduce the operating intensity level. In designing switches, the amplitude transmission coefficient τ (or amplitude coupling coefficient κ) plays a significant role. From the simulation results, smaller τ , which corresponds to stronger coupling effect, is desirable because it provides less switching intensity and larger output intensity without any expense of ON-OFF contrast. α_c is primarily contributed by the side-wall roughness. To obtain better switch performance, it needs to be as small as possible by improving fabrication technique. The size of microring is another design parameter. Although we did not plot the influence on the output versus input curve, the smaller size provides lower switching intensity because the build-up factor within the microring is proportional to the finesse, which is inversely proportional to the perimeter. The larger the build-up factor, the stronger the optical nonlinearity will be. However, the size cannot be too small because of the increase of the bending loss.

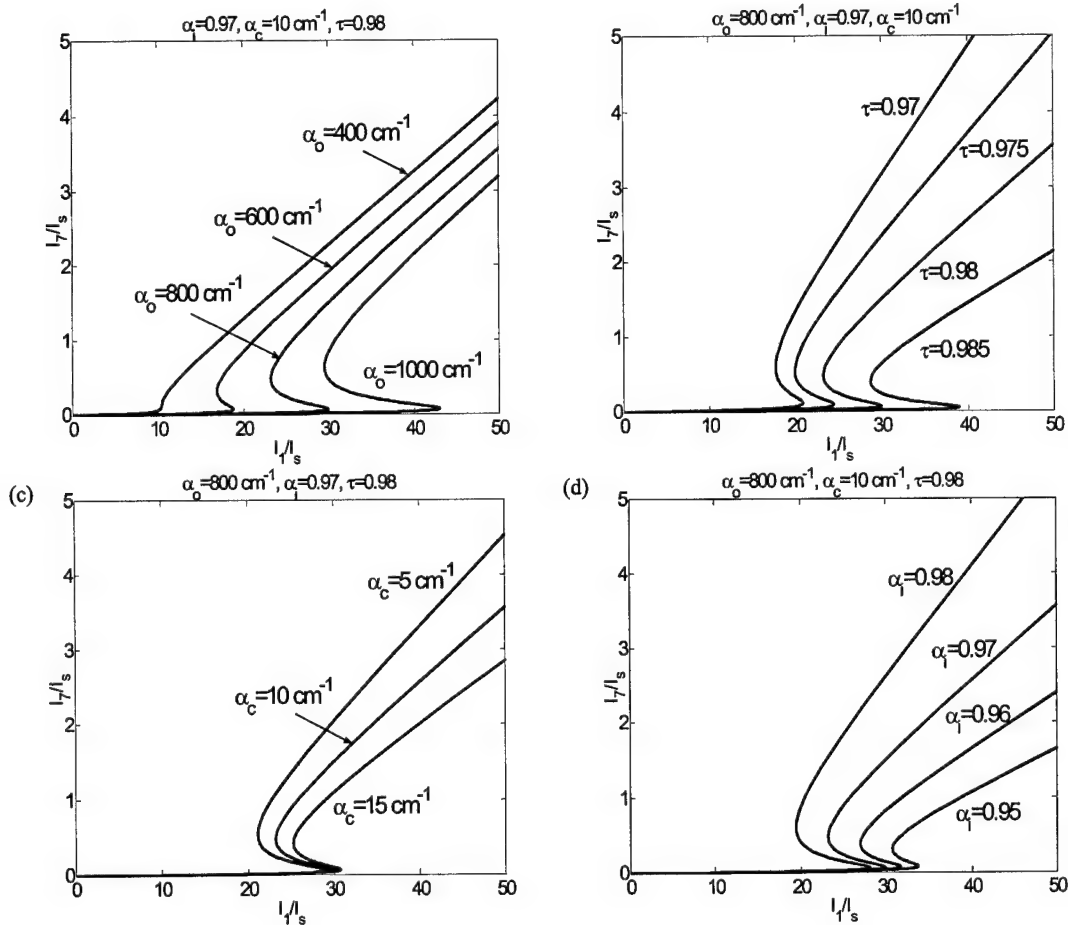


Fig. 9. Output intensity versus input intensity by changing (a) α_o ; (b) τ ; (c) α_c and (d) α_i for fixed $n_{eff}=1.6$ and $m=50$ at $\lambda=1.55\mu m$.

Our preliminary results also show that using nanoimprinting, microring and microdisk polymer structures can be fabricated.

2.4. Optical Switching of Resonant Grating Structures Fabricated by Nanoimprinted NLO Polymer

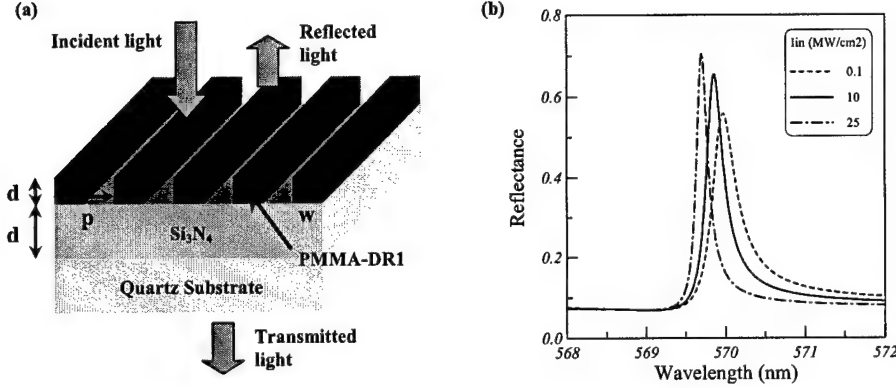


Fig. 10. (a) Schematic of the proposed optical switching device based on resonant grating waveguide structure by using nanoimprinted DR1-doped PMMA polymer grating. (b) Calculated reflectance spectra around 570 nm for grating filling ratio (w_p/p) of 0.57, where $p = 310$ nm, $d_1 = 42$ nm and $d_2 = 315$ nm.

structure has been studied extensively in the past to act as narrow band optical filters. The resonance effect is a result of the coupling of the diffracted wave by the subwavelength grating to the quasi-guided modes in the waveguide layer [19]. Because the resonant grating structure has highly sensitive frequency selectivity, we can design an optical switch by choosing the grating material to have intensity dependent refractive index. We used (DR1) functionalized PMMA in our simulation, which has been verified experimentally to possess large third-order nonlinearity and sub-ps response time [20, 21].

The resonant grating device is designed (Fig. 10a) to operate in the wavelength range of 560 ~ 580 nm where the third-order nonlinearity is high [20]. The DR1-PMMA grating layer serves to diffract the incident laser beam and the Si₃N₄ layer functions as a waveguide to support multiple propagation modes. Using rigorous coupled wave analysis, we have calculated reflectance spectra as shown in Fig. 10b. As the power of the incident laser beam changes, the refractive index of DR1-PMMA is changed due to the third-order nonlinearity. As a result, the resonant condition is simultaneously modified, resulting in the shift of resonance reflection peak. The amplitude increase in reflection peak at high input intensity is due to reduced absorption because DR1-PMMA exhibits saturable absorption behavior [20].

The simulated switching behavior between the transmittance and the reflectance as a function of incident optical intensity is shown in figure 11a for wavelength of 570 nm, and in figure 11b for 580 nm. It is also possible to design the device structure to obtain the opposite switching behavior (high transmission at low intensity and high reflection at high intensity). According to the simulation, the input intensity for switching is lower at 570 nm due to the larger third-order nonlinear coefficient, while the contrast is greater at 580 nm due to lower absorption coefficient. Even though the switching intensity at wavelength of 580 nm seems high, based on our calculation, there is no significant heat generation for short optical pulses due to the low absorption coefficient around 580 nm. It can be seen from figure 7a

In this section, we consider a new optical switching device that can be realized by using a nanoscale periodic NLO polymer structure. The basic device structure is a resonant waveguide grating, where a diffraction grating is formed on top of a slab waveguide. Such a

that the threshold intensity for switching at wavelength of 570 nm is only 10 MW/cm^2 , corresponding to the pulse energy of tens of nano-joule. Therefore, low-power optical switching can be expected.

Our simulations show that the switching characteristics depend sensitively on the dimensions of the DR1-PMMA grating structure. Such a structure can be realized by using the nanoimprinting technique described above. It should be noted that in designing the device

structure, there are various parameters that can be adjusted, such as the thickness of each layer, the grating period, and the duty cycle of the grating layer. In the experiment, incident angle as well as wavelength can also be fine tuned in order to achieve the optimal switching behavior in such a device.

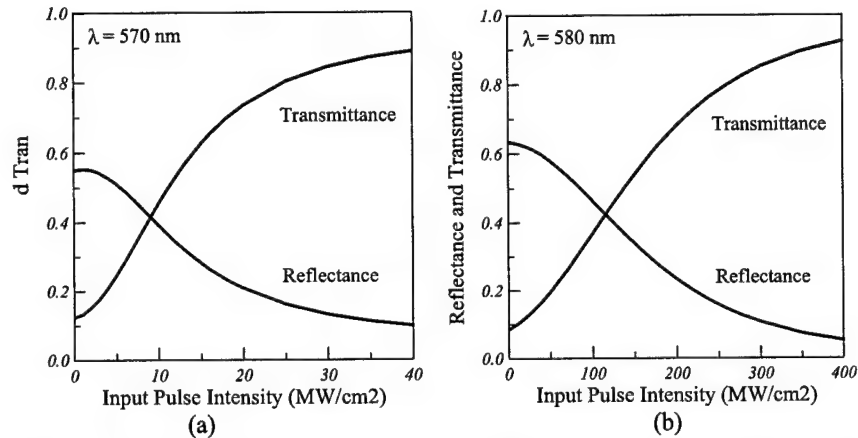


Fig. 11. (a) Calculated reflectance and transmittance as a function of input pulse intensity for wavelength (a) at 570 nm for the same device parameters as that in figure 6b, and (b) at 580 nm for grating filling ratio of 0.57, and $p = 310 \text{ nm}$, $d_1 = 44 \text{ nm}$ and $d_2 = 419 \text{ nm}$.

2.5. Tunable filter and EO modulator in PBG structure incorporated with EO polymer

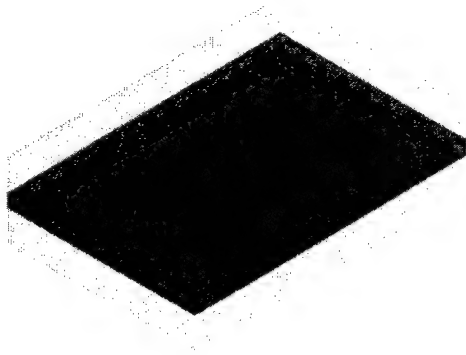


Fig. 12. (a) Schematic of perspective and cross-section view of the proposed 2D PBG defect resonator structure fabricated on SOI wafer. Waveguides are formed by removing a row of Si rods and a defect is by enlarging a Si rod. The fabricated Si rods PBG are then embedded in EO polymer, which not only provides vertical dielectric confinement, but also offers tunability by means of electro-optic effect.

In contrast to microring resonator in which Q factor is limited by intrinsic radiation losses and degrades with surface roughness, photonic crystal microcavities do not suffer from intrinsic radiation losses [22], and can be true single mode. Among the many potential applications of PBG photonics, ultracompact add/drop filter application has been proposed a few years ago by integrating PBG waveguides with defect resonator [23]. Theoretical results were obtained for 2D PBG structures made of dielectric rods that use air-line waveguides and resonators to achieve sufficient coupling between the two. However no experimental realization of such devices have been reported because in an actual 2D slab structure the optical fields will not be

confined in the vertical direction in the air-guide region. We propose a novel approach of filling the air region of a 2D rod PBG structure with EO polymers, and using an upper and lower cladding layer that has a lower refractive index than the EO polymer. A schematic of the device structure is shown in Fig. 12 with polymer waveguide as the I/O and drop port and a larger Si rod as a defect resonator. The advantage

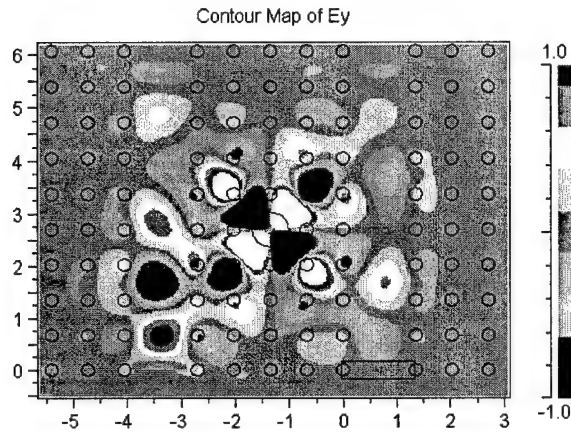


Fig. 13. Electric field plot for resonance mode. Input is single frequency continuous wave corresponding to the resonant cavity mode.

of this structure is that not only the EO polymer will provide vertical dielectric confinement needed for waveguiding, but also the device can be tuned by changing the refractive index of the polymer via EO effect. Fig. 13 is a Finite Difference Time Domain (FDTD) simulation of the optical field distribution at the resonant condition. Fig. 14 is the simulated results based on FDTD method that shows the transmission detected at the drop port as a function of the wavelength, clearly small index change can cause sufficient shift of the resonance peak. Note that the limited data points may not resolve the true resonance peak value due to the

long simulation time. We found that by blocking one side of the PBG waveguide in the dropping port, all the optical energy can be directed and the transmission amplitude doubles. For fixed input wavelength, the device can act as a very compact EO modulator.

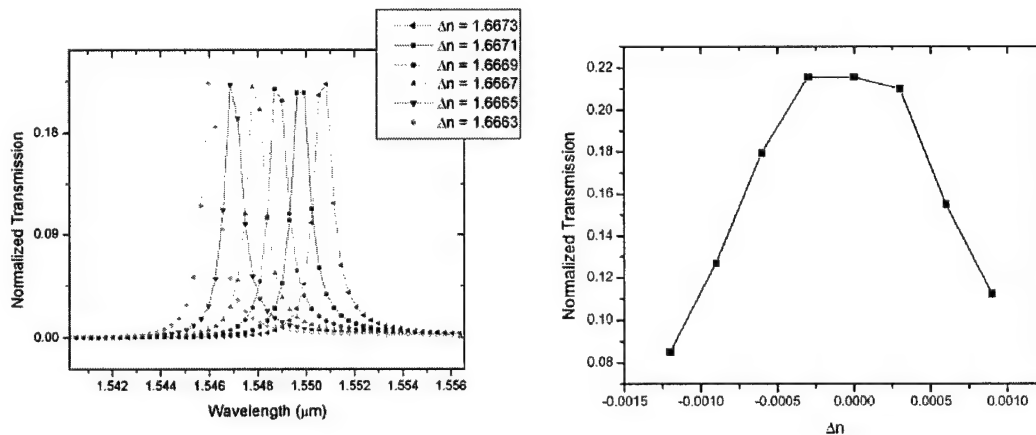


Fig. 14. Finite-difference time-domain (FDTD) simulation of the proposed 2D defect PBG structure showing tunable filter characteristics. Small change in refractive index (0.001) could cause significant change in the resonance transmission.

2.6. Enhanced fluorescence of dyes on nanostructured surfaces

In discussions between the P.I. and Prof. Boyd during the first year of this program, it became apparent that both individuals are very interested in the use of optical techniques for the biomedical diagnostic purposes and for the construction of biosensors. In fact, there is some hope that the basic microdisk resonator structure can be configured to act as a biosensor. As an additional project (at present a sideline to our basic research program, but one with significant potential) we are investigating the extent to which we can use a micro-structured (roughened) surface that are fabricated at the University of Michigan to enhance the intensity of fluorescence from organic molecules attached to the surface. As fluorescence techniques are currently used as a standard method for the sensing of various biological materials, this technique could potentially be very important. We hope that this surface enhancement might prove useful in the design of sensors of biological materials such as the sort of pathogens that might be encountered in a biological warfare situation. Prof. Boyd's group has performed experimental investigations of the use of structured surfaces to enhance the fluorescent yield of organic molecules. Some of our results are shown in Fig. 15. These data show that the fluorescent yield is several times greater from a roughened silicon surface than from a polished surface. We are presently extending this technique to determine the role of a metallic layer on top of the roughened silicon surface. Measurements are continuing to explore the conditions under which enhancement can be achieved.

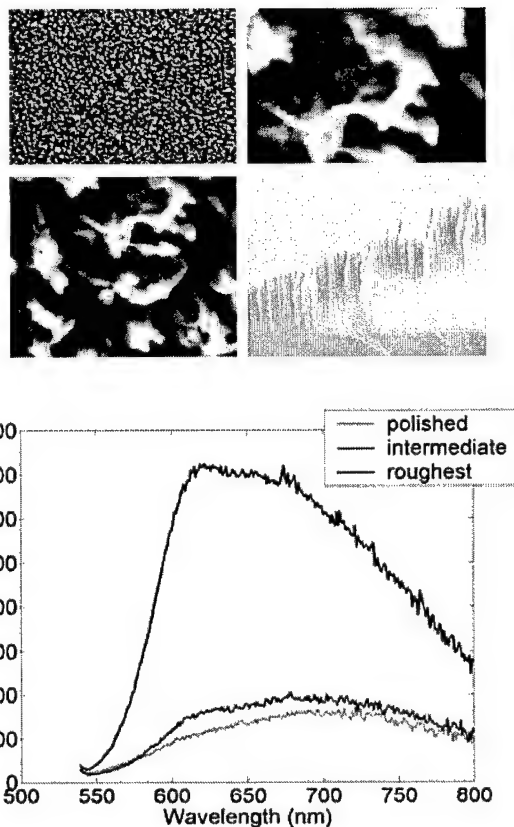


Fig. 15 Enhanced Fluorescence of Rhodamine - 6g deposited onto microstructured silicon surfaces, the SEM pictures show the surface morphology.

2.7. New measurement techniques for Nonlinear optical materials

Prof. Boyd's group are also working on the development of a new technique for measuring the nonlinear optical properties of a material system. This technique involves using recently devices techniques for measuring directly the phase of an ultrashort optical pulse. These techniques go by the acronyms FROG and SPIDER. The procedure is to measure the phase structure of a laser beam both before and after the beam propagates through a material sample. Changes in the phase can then be attributed to the response of the material sample, and by measuring the intensity dependence of these changes we are able to determine the nonlinear coefficients of the material sample. Our goal is to use this

Fig. 2. SEM pictures of (a) SiO_2 mold with trench depth of - nm thick narrow wall defines the gap distance between the two racetrack fabricated by direct imprinting method.

technique to characterize novel materials fabricated at the University of Michigan. Our initial studies of this technique have made use of the optical glass SF-59. Some laboratory results demonstrating this technique are shown in Fig. 16. In the near future we want to apply this technique to the characterization of materials including gold films, gold-doped glass, chalcogenide glasses, photonic bandgap materials, and zirconia nanoparticles suspended in glass.

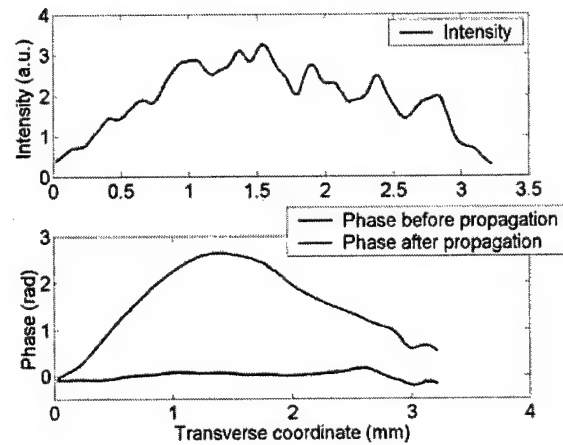


Fig. 16 Transverse intensity and phase of beams that have traveled through a SF-59 glass sample.

2.8. Polymer Micro-ring Photonic Resonator Devices

This type of devices has been studied extensively in recent years due to their important applications in integrated photonic circuits [24]. The device is typically in the form of a μ -ring closely coupled to a waveguide, and offers unique properties such as narrow bandwidth filtering, high quality factor, and compactness. Potential applications include channel add/drop filters, WDM demultiplexers, true ON-OFF switches, dispersion compensators, to name only a few. To date, most of the micro-ring resonator devices have been fabricated in semiconductor materials using a combination of electron-beam lithography and reactive ion etching (RIE). We have attempted to fabricate polymer μ -ring resonators, because we foresee that the use of polymer materials can offer a number of advantages over semiconductor-based devices. These include reducing surface roughness scattering, providing more efficient coupling to fibers, low cost and compatibility to most substrates. It also allows us to easily explore nonlinear optical effect for active devices by using many existing NLO polymers [25].

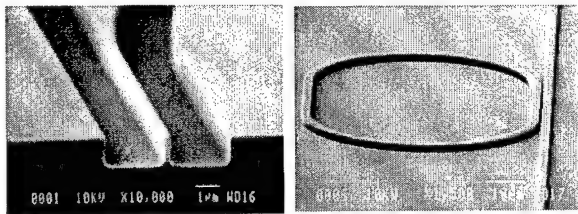


Fig. 17. SEM pictures of (a) SiO_2 mold with trench depth of $\sim 1.5 \mu\text{m}$ that is used to replicate the polymer waveguides; the 200-nm thick narrow wall defines the gap distance between the two coupled waveguides. (b) Micro-ring resonator in the shape of a racetrack fabricated by direct imprinting method.

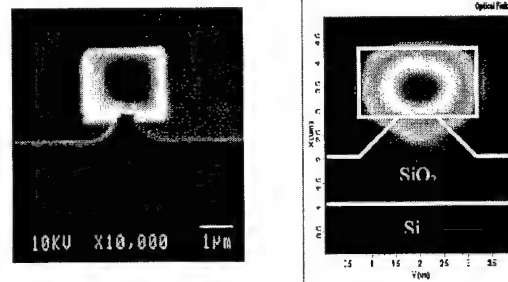


Fig. 18. (a) Cross section SEM picture of a rectangular PMMA waveguide sitting on top of a SiO_2 pedestal. (b) Simulation results showing optical field confinement in the waveguide.

We have developed two techniques to fabricate the polymer micro-ring resonator devices. The first one is direct imprinting method by using a mold with deep features. Figures 17 and 18 show the SEM pictures of the mold and the fabricated micro-ring structure (perspective view and cross-section view), as well as simulated optical confinement in the waveguide. We have used a number of polymers, including PMMA, Polystyrene and Polycarbonate. The second method is a template approach that would facilitate the fabrication of thicker polymer waveguides with reduced defects, as well as allow the use of many polymer materials that can not be directly imprinted. Details of the fabrication methods and some very recent experimental characterization results have submitted for journal publication [26].

3. Summary

This 1-year AFOSR fund has given us the opportunity to study in depth some of the concepts we have proposed as well to come up with new ideas. It also helped us to re-define our priorities as well as to re-shape the scope of our research. New photonic devices will benefit from recent developments in NLO polymers and many of the remarkable properties revealed in photonic crystal and nanocomposite structures. Such a unique combination presents great opportunities that are more than an incremental improvement over the existing material structures. We are currently exploring bio-sensing applications using these polymer based photonic devices. We hope to get continued support from AFOSR for these research programs.

4. Journal and Conference Papers

Here is a list of papers published in refereed journals and refereed conferences resulted from this grant:

Refereed Journal articles:

1. C. Y. Chao, and L. J. Guo, "Polymer Micro-ring Resonators Fabricated by Nanoimprint Technique", submitted to *J. Vac. Sci. & Technol. B*.
2. L. J. Guo, X. Cheng, and C. Y. Chao, "Fabrication of photonic nanostructures in NLO polymer," *J. Modern Optics*. Vol. 49, pp. 663-673, 2002.
3. X. Cheng, and L. J. Guo, "Electrostatic Self-assembly of Nanocomposite Polymers in Grating Structures," *J. Vac. Sci. & Technol. B*, 19, pp. 2736-2740, 2001.

Conference proceeding:

1. Y. Chao, X. Cheng, and L. J. Guo, "Nonlinear microring resonators for optical switching applications," SPIE Proceedings, Vol. 4598: Photonics Technology in the 21st century, pp. 25-35, 2001.

Refereed Conference papers:

1. C. Y. Chao, and L. J. Guo, "Polymer Micro-ring Resonators Fabricated by Nanoimprint Technique", 46th International Conference on Electron, Ion, and Photon Beam Technology and Nanofabrication, Anaheim CA, May, 2002.
2. Y. Chao, X. Cheng, and L. J. Guo, "Nonlinear microring resonators for optical switching applications," SPIE Conference: Photonics Technology in the 21st century, Singapore, Nov. 2001.

3. X. Cheng, and L. J. Guo, "Electrostatic Self-assembly of Nanocomposite Polymers in Grating Structures," 45th International Conference on Electron, Ion, and Photon Beam Technology and Nanofabrication, Washington DC, May, 2001.
4. C. Y. Chao, X. Cheng, and L. J. Guo, "Optical Switching in Resonant Grating Waveguide Structures Fabricated by Nanoimprinted NLO Polymer," 45th International Conference on Electron, Ion, and Photon Beam Technology and Nanofabrication, Washington DC, May, 2001.

Reference:

- ¹ Joannopoulos, J. D., Meade, R. D., and Winn, J. N., 1995, Photonic crystals : molding the flow of light, (Princeton, N.J. : Princeton University Press).
- ² L. J. Guo, X. Cheng, and C. Y. Chao, "Fabrication of photonic nanostructures in NLO polymer," *J. Modern Optics*. Vol. 49, pp. 663-673, 2002.
- ³ X. Cheng, and L. J. Guo, "Electrostatic Self-assembly of Nanocomposite Polymers in Grating Structures," *J. Vac. Sci. & Technol. B*, 19, pp. 2736-2740, 2001.
- ⁴ CHOU, S. Y., KRAUSS, P. R., and RENSTROM, P. J., 1996, *Science*, 272, 85.
- ⁵ S. Y. Chou, P. R. Krauss, W. Zhang, L. J. Guo, and L. Zhuang, "Sub-10 nm imprint lithography and applications," *J. Vac. Sci. Technol. B*, Vol. 15(6), pp. 2897-2904 (1997), and the references therein.
- ⁶ Guo, L. J., Krauss, P. R., and Chou, S. Y., 1997, *Appl. Phys. Lett.* 71, 1881.
- ⁷ NELSON, R. L. and BOYD, R. W., 1999, *Journal of Modern Optics*, 46, 1061.
- ⁸ YANG, X., MCBRANCH, D., SWANSON, B., and LI, D., 1995, A molecular architectural approach to second-order nonlinear optical materials, in *Thin films for integrated optics applications*, edited by B. W. Bruce, S. R. Marder, and D. M. Walba, (Pittsburgh, PA: Materials Research Society).
- ⁹ MARKS, T. J., RATNER, M. A., 1995, *Andew. Chem. Int. Ed. Engl*, 34, 155.
- ¹⁰ LIN, W., MARKS, T. J., YITZCHAIK, S., LIN, W., and WONG, G. K., 1995, New synthetic approaches to self-assembled chromophoric multilayers as second-order nonlinear optical materials, in *Thin films for integrated optics applications*, edited by B. W. Bruce, S. R. Marder, and D. M. Walba, (Pittsburgh, PA: Materials Research Society).
- ¹¹ DECHER, G., 1997, *Science*, 277, 1232.
- ¹² HEFLIN, J. R., LIU, FIGURA, Y. C., MARCIU, D., and CLAUS. R. O., 1997, SPIE Vol. 3147, 10.
- ¹³ F. Sanchez, "Optical bistability in a 2×2 coupler fiber ring resonator: parametric formulation," *Opt. Comm.* 142, pp. 211-214, 1997.
- ¹⁴ L. Luo, and P. L. Chu, "Optical bistability in a coupled fiber ring resonator system with nonlinear absorptive medium," *Opt. Comm.* 129, pp. 224-228, 1996.
- ¹⁵ L. G. Luo, R. F. Peng, and P. L. Chu, "Optical bistability in a passive erbium-doped fibre ring resonator," *Opt. Comm.* 156, pp. 275-278, 1998.
- ¹⁶ J. E. Heebner and R. W. Boyd, "Enhanced all-optical switching by use of a nonlinear fiber ring resonator," *Opt. Lett.* 24, pp. 847-849, 1999.
- ¹⁷ H. S. Nalwa, and S. Miyata, *Nonlinear Optics of Organic Molecules and Polymers*, CRC Press, New York, 1997.
- ¹⁸ C. Y. Chao, X. Cheng, and L. J. Guo, "Nonlinear microring resonators for optical switching applications," to be published in the SPIE Proc, 2001.
- ¹⁹ ROSENBLATT, D., SHARON, A., and FRIESEM, A. A., 1997, *IEEE Journal of Quantum Electronics*, 33, 2038.
- ²⁰ RANGEL-ROJO, R., YAMADA, S., and MATSUDA, H., 1998, *Appl. Phys. Lett.*, 72, 1021.
- ²¹ LEDNEV, I. K., YE, T. -Q., HESTER, R. E., and MOORE, J. N. 1996, *J. Phys. Chem.*, 100, 13338.

-
- ²² S. Fan, P. R. Villeneuve, and J.D. Joannopoulos, "Microcavities in photonic crystals: mode symmetry, tenability and coupling efficiency," *Phys. Rev. B* **54**, 7837 (1996).
- ²³ S. Fan, P. R. Villeneuve, J. D. Joannopoulos, and H. A. Haus, "Channel drop filters in photonic crystals," *Opt. Express*, vol. 4, July 6, 1998.
- ²⁴ B. E. Little, and S. T. Chu, *Optics & Photonics News*, **11**, 24, (2000), and references therein.
- ²⁵ Y. Chao, X. Cheng, and L. J. Guo, *SPIE Proceedings*, Vol. 4598, 25, (2001).
- ²⁶ Y. Chao, and L. J. Guo, submitted to *J. Vac. Sci. Technol. B* (2002).